

# Phenomenological consequences of four zero neutrino Yukawa textures

Sandhya Choubey<sup>a</sup> , Werner Rodejohann<sup>b</sup> , Probir Roy<sup>c\*</sup>

<sup>a</sup>*Harish-Chandra Research Institute,  
Chhatnag Road, Jhansi, Allahabad 211019, India*

<sup>b</sup>*Max-Planck-Institut für Kernphysik,  
Postfach 103980, D-69029 Heidelberg, Germany*

<sup>\*</sup>*DAE Raja Ramanna Fellow*

<sup>c</sup>*Saha Institute of Nuclear Physics,  
Block AF, Sector 1, Kolkata 700 064, India*

## Abstract

For type I seesaw and in the basis where the charged lepton and heavy right-handed neutrino mass matrices are real and diagonal, four has been shown to be the maximum number of zeros allowed in the neutrino Yukawa coupling matrix  $Y_\nu$ . These four zero textures have been classified into two distinct categories. We investigate certain phenomenological consequences of these textures within a supersymmetric framework. This is done by using conditions implied on elements of the neutrino Majorana mass matrix for textures of each category in  $Y_\nu$ . These conditions turn out to be stable under radiative corrections. Including the effective mass, which appears in neutrinoless double beta decay, along with the usual neutrino masses, mixing angles and phases, it is shown analytically and through scatter plots how restricted regions in the seesaw parameter space are selected by these conditions. We also make consequential statements on the yet unobserved radiative lepton flavor violating decays such as  $\mu \rightarrow e\gamma$ . All these decay amplitudes are proportional to the moduli of entries of the neutrino Majorana mass matrix. We also show under which conditions the low energy CP violation, showing up in neutrino oscillations, is directly linked to the CP violation required for producing successful flavor dependent and flavor independent lepton asymmetries during leptogenesis.

# 1 Introduction

Neutrino mixing, leptogenesis and (in a supersymmetric framework) radiative lepton flavor violating decays ( $\ell_i \rightarrow \ell_j \gamma$ ),  $\ell$  being a charged lepton and  $i, j$  being generation indices, have generally been acknowledged [1] as important tools to constrain parts of the seesaw [2] parameter space. Any study of these tools gets considerably facilitated by the assumption of texture zeros being present in the Yukawa coupling matrix  $Y_\nu = m_D/v_u$  [3–6]. Here  $v_u$  is the vev of the up-type Higgs and  $m_D$  is the Dirac neutrino mass matrix. Texture zeros also help in relating [3–6] CP violation at low energies to that required for leptogenesis. Given the observed pattern of neutrino mixing and assuming no neutrino to be exactly massless, four is now known [7] to be the maximum number of zeros allowed in  $m_D$  within the type I seesaw framework. More zero entries in  $Y_\nu$  lead [7] to at least one completely unmixed neutrino. This statement is made, of course, in the standard weak basis where the right-handed neutrino and charged lepton mass matrices,  $M_R$  and  $m_\ell$  respectively, are real and diagonal. All such allowed four zero textures in  $m_D$  have been completely classified [7]. Our aim in this work is to study the implications of these allowed and completely classified four zero textures for radiative lepton flavor violating decays as well as for leptogenesis. We shall also make observations on related aspects of neutrino mixing and neutrinoless double beta decay.

In type I seesaw [2] the low energy neutrino mass matrix in family space obeys the ‘matching condition’

$$m_\nu = -m_D M_R^{-1} m_D^T = U m_\nu^{\text{diag}} U^T, \quad (1)$$

where  $U$  is the PMNS matrix, parameterizable in terms of three angles  $\theta_{12}, \theta_{23}, \theta_{13}$  and three phases  $\alpha, \beta, \delta$ . Thus,

$$U = \begin{pmatrix} c_{12} c_{13} & s_{12} c_{13} & s_{13} e^{-i\delta} \\ -c_{23} s_{12} - s_{23} s_{13} c_{12} e^{i\delta} & c_{23} c_{12} - s_{23} s_{13} s_{12} e^{i\delta} & s_{23} c_{13} \\ s_{23} s_{12} - c_{23} s_{13} c_{12} e^{i\delta} & -s_{23} c_{12} - c_{23} s_{13} s_{12} e^{i\delta} & c_{23} c_{13} \end{pmatrix} P, \quad (2)$$

where  $c_{ij} = \cos \theta_{ij}$ ,  $s_{ij} = \sin \theta_{ij}$ ,  $\delta$  is the Dirac-type CP-violating phase and the Majorana phases  $\alpha$  and  $\beta$  are contained in the matrix  $P = \text{diag}(1, e^{i\alpha}, e^{i(\beta+\delta)})$ . Leptonic CP violation, that can show up in neutrino oscillation experiments, can be described through a rephasing (Jarlskog) invariant quantity given by [6]

$$J_{\text{CP}} = \text{Im} \left\{ U_{e1} U_{\mu 2} U_{e2}^* U_{\mu 1}^* \right\} = -\frac{\text{Im} \{ h_{12} h_{23} h_{31} \}}{\Delta m_{21}^2 \Delta m_{31}^2 \Delta m_{32}^2}, \quad \text{where } h = m_\nu m_\nu^\dagger. \quad (3)$$

With the parameterization of Eq. (2), one has  $J_{\text{CP}} = \frac{1}{8} \sin 2\theta_{12} \sin 2\theta_{23} \sin 2\theta_{13} \cos \theta_{13} \sin \delta$ . Whereas the presence or the value of any of the phases is currently unknown, the oscillation parameters are constrained as follows [8] (see also [9]):

$$\Delta m_{21}^2 = 7.67_{-0.21}^{+0.22} \left( {}_{-0.61}^{+0.67} \right) \times 10^{-5} \text{ eV}^2,$$

$$\begin{aligned}
\Delta m_{31}^2 &= \begin{cases} -2.37 \pm 0.15 \begin{pmatrix} +0.43 \\ -0.46 \end{pmatrix} \times 10^{-3} \text{ eV}^2 & (\text{inverted ordering}), \\ +2.46 \pm 0.15 \begin{pmatrix} +0.47 \\ -0.42 \end{pmatrix} \times 10^{-3} \text{ eV}^2 & (\text{normal ordering}), \end{cases} \\
\sin^2 \theta_{12} &= 0.32 \pm 0.02 \begin{pmatrix} +0.08 \\ -0.06 \end{pmatrix}, \\
\sin^2 \theta_{23} &= 0.45 \begin{matrix} +0.09 \\ -0.06 \end{matrix} \begin{pmatrix} +0.19 \\ -0.13 \end{pmatrix}, \\
\sin^2 \theta_{13} &= 0.0 \begin{matrix} +0.019 \\ -0.000 \end{matrix} \begin{pmatrix} +0.05 \\ -0.00 \end{pmatrix}.
\end{aligned} \tag{4}$$

The  $1\sigma$  ( $3\sigma$ ) ranges around the best-fit values have been given above.

As in Ref. [7], we consider textures in  $m_D$  in the basis in which both  $m_\ell = \text{diag}(m_e, m_\mu, m_\tau)$  and  $M_R = \text{diag}(M_1, M_2, M_3)$  are real and diagonal. All flavor mixing information is thus encoded in the Dirac mass matrix  $m_D$ . The latter can be written in the most general form as

$$m_D = \begin{pmatrix} a_1 e^{i\alpha_1} & a_2 e^{i\alpha_2} & a_3 e^{i\alpha_3} \\ b_1 e^{i\beta_1} & b_2 e^{i\beta_2} & b_3 e^{i\beta_3} \\ c_1 e^{i\gamma_1} & c_2 e^{i\gamma_2} & c_3 e^{i\gamma_3} \end{pmatrix}. \tag{5}$$

Here, for each entry, we have listed the real amplitude ( $a_i, b_i, c_i$ ) and the corresponding phase ( $\alpha_i, \beta_i, \gamma_i$ ) explicitly. Of course, three of the phases (one per row) can be rephased away. This Dirac mass matrix can also be expressed as [10]

$$m_D = iU \sqrt{m_\nu^{\text{diag}}} R \sqrt{M_R}, \tag{6}$$

where  $R$  is a complex, orthogonal matrix. This Casas-Ibarra parametrization illustrates an important feature: even when the elements of  $m_\nu$  and  $M_R$  are known, there is still an infinite number of Dirac mass matrices leading to the observed low energy phenomenology. Other observables need to be used in order to break this degeneracy [11].

A well-known strategy to distinguish between different models, leading to the same low energy neutrino data, is to make use of Lepton Flavor Violation (LFV) and leptogenesis. LFV in supersymmetric seesaw scenarios leads to loop-induced decays such as  $\ell_i \rightarrow \ell_j \gamma$ , with flavor indices  $i, j$  spanning ( $1 = e, 2 = \mu, 3 = \tau$ ), with the constraint  $i > j$ . In mSUGRA scenarios, with universal boundary conditions for scalar sparticle mass matrices, one obtains the one-loop relation [12]

$$\text{BR}(\ell_i \rightarrow \ell_j + \gamma) = (\text{const}) \text{BR}(\ell_i \rightarrow \ell_j \nu \bar{\nu}) |(m_D L m_D^\dagger)_{ij}|^2, \tag{7}$$

where the diagonal matrix  $L$  is defined as

$$L_{kl} = \ln \frac{M_X}{M_k} \delta_{kl}, \tag{8}$$

with  $M_k$  being the mass of the  $k^{\text{th}}$  right-handed neutrino. The logarithmic coefficient in the RHS of Eq. (8) takes into account the effect of renormalization group running from a high

scale  $M_X$  to the scale of the respective heavy neutrino masses. The normalization factor  $\text{BR}(\ell_i \rightarrow \ell_j \nu \bar{\nu})$  in the definition of the branching ratios in Eq. (7) is noteworthy. The relevant numbers here are  $\text{BR}(\tau \rightarrow e \nu \bar{\nu}) = 0.178$  and  $\text{BR}(\tau \rightarrow \mu \nu \bar{\nu}) = 0.174$  [13], respectively. For our later numerical work, we will ignore the small difference between the two. We will also take  $\text{BR}(\mu \rightarrow e \nu \bar{\nu})$  to be unity. Current upper limits on the branching ratios for  $\ell_i \rightarrow \ell_j \gamma$  are as follows:  $\text{BR}(\mu \rightarrow e \gamma) \leq 1.2 \times 10^{-11}$  [14],  $\text{BR}(\tau \rightarrow e \gamma) \leq 1.1 \times 10^{-7}$  [15] and  $\text{BR}(\tau \rightarrow \mu \gamma) \leq 6.8 \times 10^{-8}$  [16]. One expects these bounds to improve by two to three orders of magnitude for  $\text{BR}(\mu \rightarrow e \gamma)$  [17] and by one to two orders of magnitude for the other branching ratios [18] in the foreseeable future. The unspecified constant in the RHS of Eq. (7) depends on certain supersymmetry breaking parameters of mSUGRA, specifically the universal scalar and gaugino masses and the universal trilinear scalar coupling as well as on  $\tan \beta$ . However, we are not interested here in the exact magnitude of the branching ratios. We shall instead study the vanishing of certain branching ratios which for  $\ell_i \rightarrow \ell_j + \gamma$  turn out to be proportional to the square of the  $i, j$ th element of the low energy mass matrix  $m_\nu$ .

In principle, the above analysis could be extended also to other lepton flavor violating processes, such as  $\mu$ - $e$  conversion in nuclei [19]. Current experimental limits on this process, however, are expected to be improved considerably only much after stronger limits on  $\ell_i \rightarrow \ell_j \gamma$  have been made available. If the photon penguin contribution dominates the LFV diagrams, as happens for the case under study, a good estimate for the ratio of  $\text{BR}(\mu \rightarrow e \gamma)$  to the rate of  $\mu$ - $e$  conversion is  $\mathcal{O}(1/\alpha)$ , where  $\alpha$  is the electromagnetic fine structure constant. In particular, the rate of  $\mu$ - $e$  conversion is also proportional to  $(m_D L m_D^\dagger)_{12}$ . Hence, if in one of the scenarios to be discussed  $\text{BR}(\mu \rightarrow e \gamma)$  vanishes,  $\mu$ - $e$  conversion will be absent as well. Note, moreover, that since only one conversion channel ( $\mu \rightarrow e$ ) is experimentally accessible for the conversion process, no potentially testable double ratios can be given. For these reasons, our focus here is on the  $\ell_i \rightarrow \ell_j \gamma$  decays.

The other important aspect of seesaw phenomenology is leptogenesis. Of particular interest are the decay asymmetries [20, 21] that depend explicitly on the charged lepton flavor:

$$\begin{aligned} \varepsilon_i^\alpha &\equiv \frac{\Gamma(N_i \rightarrow \phi \bar{l}_\alpha) - \Gamma(N_i \rightarrow \phi^\dagger l_\alpha)}{\sum_\beta \left[ \Gamma(N_i \rightarrow \phi \bar{l}_\beta) + \Gamma(N_i \rightarrow \phi^\dagger l_\beta) \right]} \\ &= \frac{1}{8\pi v_u^2} \frac{1}{(m_D^\dagger m_D)_{ii}} \sum_{j \neq i} \left( \mathcal{I}_{ij}^\alpha f(M_j^2/M_i^2) + \mathcal{J}_{ij}^\alpha \frac{1}{1 - M_j^2/M_i^2} \right), \end{aligned} \quad (9)$$

where

$$\mathcal{I}_{ij}^\alpha = \text{Im} \left[ (m_D^\dagger)_{i\alpha} (m_D)_{\alpha j} (m_D^\dagger m_D)_{ij} \right], \quad \mathcal{J}_{ij}^\alpha = \text{Im} \left[ (m_D^\dagger)_{i\alpha} (m_D)_{\alpha j} (m_D^\dagger m_D)_{ji} \right]. \quad (10)$$

It is evident that  $\mathcal{I}_{ij}^\alpha = -\mathcal{I}_{ji}^\alpha$  and  $\mathcal{J}_{ij}^\alpha = -\mathcal{J}_{ji}^\alpha$ . In the MSSM, the function  $f(x)$  has the form [22]

$$f(x) = \sqrt{x} \left[ \frac{2}{1-x} - \ln \left( \frac{1+x}{x} \right) \right]. \quad (11)$$

We have given quite general expressions above for the decay asymmetries that can accommodate any nontrivial role played by flavor effects [24]. Thus  $\varepsilon_i^\alpha$  describes the decay of a heavy right-handed neutrino of mass  $M_i$  into a charged lepton of flavor  $\alpha = e, \mu, \tau$ . When the lowest-mass heavy neutrino is much lighter than the other two, i.e.  $M_1 \ll M_{2,3}$ , the lepton asymmetry is dominated by the decay of this lightest of the heavy neutrinos. In this case  $f(M_j^2/M_1^2) \simeq -3 M_1/M_j$ . Moreover, only the first term proportional to  $\mathcal{I}_{1j}^\alpha$  in Eq. (9) is relevant then since the second term proportional to  $\mathcal{J}_{ij}^\alpha$  is suppressed by an additional power of  $M_1/M_j$ . Note furthermore that the second term in Eq. (9) vanishes when one sums over flavors to obtain the flavor independent decay asymmetry:

$$\begin{aligned} \varepsilon_i &= \sum_\alpha \varepsilon_i^\alpha \equiv \frac{\sum_\alpha [\Gamma(N_i \rightarrow \phi \bar{l}_\alpha) - \Gamma(N_i \rightarrow \phi^\dagger l_\alpha)]}{\sum_\beta [\Gamma(N_i \rightarrow \phi \bar{l}_\beta) + \Gamma(N_i \rightarrow \phi^\dagger l_\beta)]} \\ &= \frac{1}{8\pi v_u^2} \frac{1}{(m_D^\dagger m_D)_{ii}} \sum_{j \neq i} \text{Im} [(m_D^\dagger m_D)_{ij}^2] f(M_j^2/M_i^2) \\ &= \frac{1}{8\pi v_u^2} \frac{1}{(m_D^\dagger m_D)_{ii}} \mathcal{I}_{ij}, \end{aligned} \quad (12)$$

where we have defined

$$\mathcal{I}_{ij} = \sum_\alpha \mathcal{I}_{ij}^\alpha. \quad (13)$$

We note here already that for all 72 four zero textures that we study the  $\mathcal{J}_{1j}^\alpha$  vanish. The expressions given above for the decay asymmetries are valid for the MSSM. Their flavor structure is, however, identical to that of just the Standard Model.

Equally important in leptogenesis are effective mass parameters that are responsible for the wash-out. We assume that a single heavy neutrino of mass  $M_1$  is relevant for leptogenesis. Then every decay asymmetry  $\varepsilon_1^\alpha$  gets washed out by an effective mass

$$\tilde{m}_1^\alpha = \frac{(m_D^\dagger)_{1\alpha} (m_D)_{\alpha 1}}{M_1}. \quad (14)$$

Moreover, the wash-out can be estimated by inserting this effective mass in the function [25]

$$\eta(x) \simeq \left( \frac{8.25 \times 10^{-3} \text{ eV}}{x} + \left( \frac{x}{2 \times 10^{-4} \text{ eV}} \right)^{1.16} \right)^{-1}. \quad (15)$$

The summation of  $\tilde{m}_1^\alpha$  over the flavor index  $\alpha$  yields  $\tilde{m}_1$ , which is the relevant parameter for the wash-out of  $\varepsilon_1$ . The final baryon asymmetry is [23–25]

$$Y_B \simeq \begin{cases} -0.01 \varepsilon_1 \eta(\tilde{m}_1) & \text{one-flavor,} \\ -0.003 \left( (\varepsilon_1^e + \varepsilon_1^\mu) \eta \left( \frac{417}{589} (\tilde{m}_1^e + \tilde{m}_1^\mu) \right) + \varepsilon_1^\tau \eta \left( \frac{390}{589} \tilde{m}_1^\tau \right) \right) & \text{two-flavor,} \\ -0.003 \left( \varepsilon_1^e \eta \left( \frac{151}{179} \tilde{m}_1^e \right) + \varepsilon_1^\mu \eta \left( \frac{344}{537} \tilde{m}_1^\mu \right) + \varepsilon_1^\tau \eta \left( \frac{344}{537} \tilde{m}_1^\tau \right) \right) & \text{three-flavor.} \end{cases} \quad (16)$$

Here we have given separate expressions for one-, two- and three-flavored leptogenesis. The three-flavor case occurs for  $M_1 (1 + \tan^2 \beta) \leq 10^9$  GeV, the one-flavor case for  $M_1 (1 + \tan^2 \beta) \geq 10^{12}$  GeV, and the two-flavor case (with the tau-flavor decoupling first and the sum of electron- and muon-flavors, which act indistinguishably) applies in between.

LFV and leptogenesis provide means of breaking degeneracies in the seesaw parameter space. This comes about since their dependence on the seesaw parameters is complementary to that of  $m_\nu$ . A related issue is the question of circumstances under which there is a connection between high and low energy CP violation, i.e., between the phases responsible for leptogenesis and the ones responsible for CP asymmetries in neutrino oscillations. Inasmuch as texture zeros simplify this process, the motivation behind the present study is to phenomenologically investigate the extent of this degeneracy breaking for all allowed Dirac mass matrices with four zero textures classified in [7]. The rest of the paper is organized as follows: in Section 2 the two categories, (i) and (ii), of the four zero textures in  $m_D$  are recapitulated and the radiative stability of the corresponding conditions on  $m_\nu$  is emphasized. In Section 3 we discuss the phenomenology of these textures, focusing on lepton mixing and the ratio of ratios in radiative LFV decays as well as on leptogenesis, wash-out factors and the basis invariant Jarlskog CP-violating parameter  $J_{\text{CP}}$ ; subsections 3.1 and 3.2 cover categories (i) and (ii) respectively. The final Section 4 contains a summary of our results and conclusions derived therefrom.

## 2 The Two Categories of Four Zero Textures

It will be helpful to provide first a summary of the classification of the four zero textures. As enumerated in Ref. [7], there are 72 allowed textures of this kind:

- (i) 54 textures in which two rows of  $m_D$  are orthogonal element by element. They can be further divided into three subclasses containing 18 matrices each:

- (ia) 18 textures in which the first and second row are orthogonal element by element, resulting in

$$(m_\nu)_{12} = (m_\nu)_{21} = 0, \quad (17)$$

i.e., the vanishing of the off-diagonal 12 (or  $e\mu$ ) entry of the effective neutrino Majorana mass matrix;

- (ib) 18 textures in which the first and third row are orthogonal element by element, resulting in the vanishing off-diagonal element condition

$$(m_\nu)_{13} = (m_\nu)_{31} = 0, \quad (18)$$

i.e., the vanishing of the off-diagonal 13 (or  $e\tau$ ) entry of the effective neutrino Majorana mass matrix;

- (ic) 18 textures in which the second and third row are orthogonal element by element, resulting in

$$(m_\nu)_{23} = (m_\nu)_{32} = 0, \quad (19)$$

i.e., the vanishing of the off-diagonal 23 (or  $\mu\tau$ ) entry of the effective neutrino Majorana mass matrix;

- (ii) 18 textures in which two columns of  $m_D$  are orthogonal element by element. They can be further divided into three subclasses containing 6 matrices each:

- (iia) 6 textures with two zeros in the first row, resulting in the vanishing sub-determinant conditions

$$|(m_\nu)_{11} (m_\nu)_{23}| - |(m_\nu)_{21} (m_\nu)_{13}| = \arg \{(m_\nu)_{11} (m_\nu)_{23} (m_\nu)_{21}^* (m_\nu)_{13}^*\} = 0 ; \quad (20)$$

- (iib) 6 textures with two zeros in the second row, resulting in the vanishing sub-determinant conditions

$$|(m_\nu)_{22} (m_\nu)_{13}| - |(m_\nu)_{12} (m_\nu)_{23}| = \arg \{(m_\nu)_{22} (m_\nu)_{13} (m_\nu)_{12}^* (m_\nu)_{23}^*\} = 0 ; \quad (21)$$

- (iic) 6 textures with two zeros in the third row, resulting in the vanishing sub-determinant conditions

$$|(m_\nu)_{33} (m_\nu)_{12}| - |(m_\nu)_{13} (m_\nu)_{32}| = \arg \{(m_\nu)_{33} (m_\nu)_{12} (m_\nu)_{13}^* (m_\nu)_{32}^*\} = 0 . \quad (22)$$

We now wish to comment on the question of the dependence of such results, as presented above, on the energy scale. In general, elements of the matrix  $Y_\nu$  change with energy in a coupled way due to radiative corrections leading to renormalization group (RG) running. Thus an element, which vanishes at low energies, can certainly develop a significant nonzero value at a very high energy. Our postulate is that four zeros are present in  $Y_\nu$  at energies relevant to oscillation experiments. Within a reasonable accuracy, such can also be taken to be the case then for radiative LFV decays. This assumption is, however, generally not valid for leptogenesis which we take to operate at  $M_1 \geq 10^9$  GeV. In a grand unified theory, of course,  $Y_\nu$  would originate at  $M_X \simeq 10^{16}$  GeV and would need to be evolved down to an energy scale below the  $Z$ -mass  $m_Z$ . If texture zeros are due to some (yet unknown) flavor symmetry at some high scale, one would need to assume that the said zeros are protected by the same symmetry during the RG running. If such is the case, our statements would continue to hold without modification.

Let us nevertheless point out a particularly interesting feature of the consequences for the neutrino Majorana mass matrix of the textures in  $m_D$  under consideration. These conditions on  $m_\nu$  are stable under RG running. If one performs the running from the high

scale  $M_X$  to the low scale  $m_Z$ , then for  $m_\nu$  this can be taken into account by multiplying each matrix element  $(m_\nu)_{ij}$  by a factor [27]. The latter is given by  $(1 + \epsilon_i)(1 + \epsilon_j)$ , where

$$\epsilon_i = c \frac{m_i^2}{16\pi^2 v^2} \ln \frac{M_X}{m_Z}$$

with  $m_{3,2,1} = m_{\tau,\mu,e}$  being the charged lepton masses. The parameter  $c$  is given by 3/2 in the SM and by  $-(1 + \tan^2 \beta)$  in the MSSM. The multiplicative nature of this correction ensures that a vanishing element of  $m_\nu$  stays vanishing. Thus the consequence for  $m_\nu$  of every texture under category (i) is safe under RG running. It is, additionally, rather surprising that the corresponding consequences for  $m_\nu$  from all textures in category (ii) are also unharmed by the RG running from radiative corrections. For instance, consider category (iia) and perform the corrections in condition (20). The multiplication of  $(m_\nu)_{ij}$  with the factors  $(1 + \epsilon_i)(1 + \epsilon_j)$  leads to

$$\begin{aligned} & |(m_\nu)_{11}(m_\nu)_{23}| - |(m_\nu)_{21}(m_\nu)_{13}| \rightarrow |(m_\nu)'_{11}(m_\nu)'_{23}| - |(m_\nu)'_{21}(m_\nu)'_{13}| \\ & = |(m_\nu)_{11}(m_\nu)_{23}|(1 + \epsilon_1)^2(1 + \epsilon_2)(1 + \epsilon_3) - |(m_\nu)_{21}(m_\nu)_{13}|(1 + \epsilon_1)(1 + \epsilon_2)(1 + \epsilon_1)(1 + \epsilon_3) \\ & = (1 + \epsilon_1)^2(1 + \epsilon_2)(1 + \epsilon_3) (|(m_\nu)_{11}(m_\nu)_{23}| - |(m_\nu)_{21}(m_\nu)_{13}|), \end{aligned}$$

so that condition (20) remains unchanged. The result is identical for categories (iib) and (iic), the matrix indices 1, 2, 3 appearing the same number of times on both sides of the conditions (21) and (22). This defines an interesting class of ‘‘RG invariants’’.

## 3 The Phenomenology of Four Zero Textures

### 3.1 Category (i)

We first discuss some general issues concerning the phenomenology of the textures under consideration. To start with, take the subclass in category (i) in which rows  $i$  and  $j$  ( $\neq i$ ) of  $m_D$  are orthogonal, element by element:

$$(m_\nu)_{ij} = (m_\nu)_{ji} = 0. \quad (23)$$

It also follows that for this subclass of four zero textures,

$$(m_D K m_D^\dagger)_{ij} = 0, \quad (24)$$

where  $K$  is any diagonal matrix. The immediate implication is that the branching ratio for the decay  $\ell_i \rightarrow \ell_j \gamma$  is zero for these textures:

$$\text{BR}(\ell_i \rightarrow \ell_j \gamma) = 0. \quad (25)$$

Therefore all such textures of  $m_D$  would be excluded by any future experimental observation of this decay mode<sup>1</sup>.

---

<sup>1</sup>The requirement of a vanishing  $(m_D m_D^\dagger)_{12}$  can lead via 2-loop effects to a lower limit on  $\text{BR}(\mu \rightarrow e \gamma)$ , connected to the product of the branching ratios of  $\tau \rightarrow \mu \gamma$  and  $\tau \rightarrow e \gamma$  [26]. Obviously the 2-loop induced branching ratio is very small.

Another interesting feature is that, in the textures of category (i) and for an arbitrary  $j \neq i$ , the relation

$$|(m_D L m_D^\dagger)_{ij}| \propto |(m_\nu)_{ij}| \quad (26)$$

holds. However, it is not possible to construct predictive ratios of branching ratios from this, unless the heavy neutrino masses are known. Consider as an example the texture

$$m_D = \begin{pmatrix} 0 & a_2 & a_3 e^{i\alpha_3} \\ b_1 & 0 & 0 \\ c_1 & c_2 e^{i\gamma_2} & 0 \end{pmatrix}, \quad (27)$$

which belongs to category (ia) and leads to  $(m_\nu)_{12} = \text{BR}(\mu \rightarrow e\gamma) = 0$ . The non-zero branching ratios for the decays  $\tau \rightarrow e\gamma$  and  $\tau \rightarrow \mu\gamma$  are governed by

$$|(m_D L m_D^\dagger)_{13}|^2 = a_2^2 c_2^2 L_2^2 \quad \text{and} \quad |(m_D L m_D^\dagger)_{23}|^2 = b_1^2 c_1^2 L_1^2, \quad (28)$$

respectively. The low energy Majorana mass matrix is

$$m_\nu = - \begin{pmatrix} \frac{a_2^2}{M_2} + \frac{a_3^2 e^{2i\alpha_3}}{M_3} & 0 & \frac{a_2 c_2 e^{i\gamma_2}}{M_2} \\ \cdot & \frac{b_1^2}{M_1} & \frac{b_1 c_1}{M_1} \\ \cdot & \cdot & \frac{c_1^2}{M_1} + \frac{c_2^2 e^{2i\gamma_2}}{M_2} \end{pmatrix}. \quad (29)$$

It follows that

$$\frac{\text{BR}(\tau \rightarrow e\gamma)}{\text{BR}(\tau \rightarrow \mu\gamma)} = \frac{|(m_\nu)_{13}|^2}{|(m_\nu)_{23}|^2} \left( \frac{M_2 L_2}{M_1 L_1} \right)^2. \quad (30)$$

Without any further information about the heavy neutrino masses, one is unable to predict this ratio. The same feature is valid for all textures in category (i). We will not work out here all 72 possibilities.

Leptogenesis – either of the unflavored or of the flavor dependent variety – is quite possible in general for such textures. As mentioned earlier, we work under the assumption that  $M_1 \ll M_{2,3}$  so that one needs to consider only the decay of  $N_1$ . Thus, among the parameters responsible for leptogenesis,  $i$  is always 1. Generalization to the more general situation, including  $M_{2,3}$  is, however, straightforward. It turns out that for the textures under study here all  $\mathcal{J}_{1j}^\alpha$  vanish and we are left only with the  $\mathcal{I}_{1j}^\alpha$ . Specific textures in this subclass will of course have some of the  $\mathcal{I}_{ij}^\alpha$  zero in case the appropriate elements of  $m_D$  happen to lead to this. In the example from Eq. (27) the only non-zero decay asymmetry is

$$\mathcal{I}_{12}^\tau = c_1^2 c_2^2 \sin 2\gamma_2. \quad (31)$$

It is interesting to ask under what circumstances the “leptogenesis phase”  $\gamma_2$  is responsible for low energy leptonic CP violation as well. Evaluating the invariant in Eq. (3), which

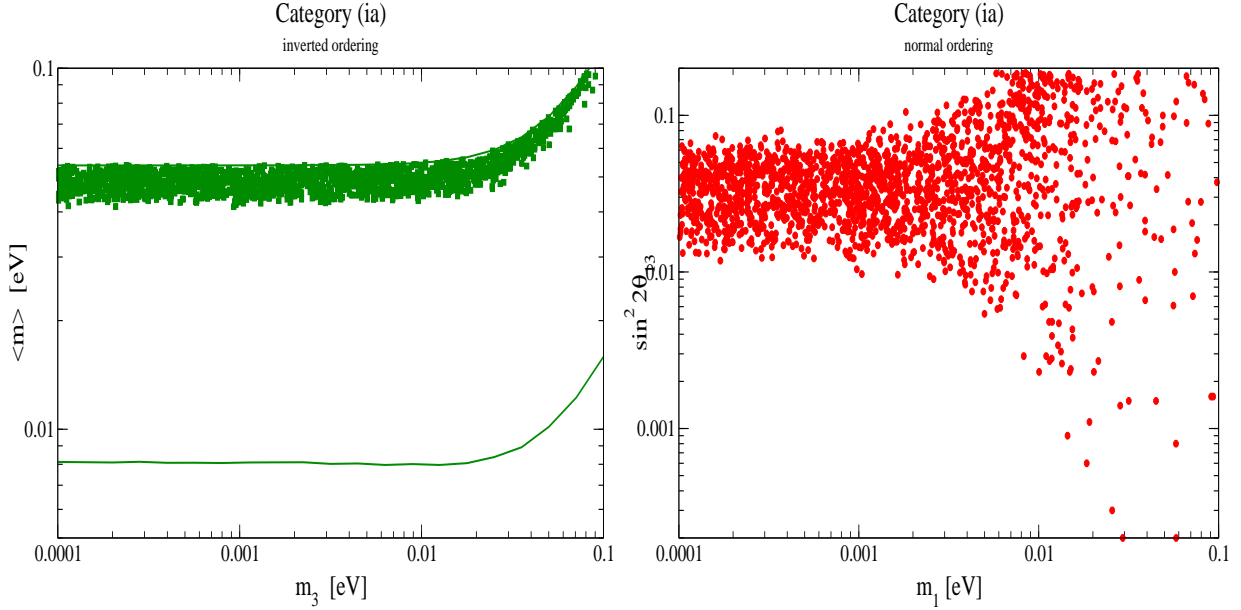


Figure 1: Category (ia) or  $(m_\nu)_{12} = 0$ : scatter plots of the effective mass versus the smallest mass in case of an inverted mass ordering (left) and of  $\sin^2 2\theta_{13}$  versus the smallest mass for a normal mass ordering (right). For the first plot we have also given the general upper and lower limit of the effective mass when the currently allowed  $3\sigma$  values of the oscillation parameters are used. The corresponding plots for category (ib) look basically identical.

describes CP violation in neutrino oscillations, gives

$$\Delta m_{21}^2 \Delta m_{31}^2 \Delta m_{32}^2 J_{\text{CP}} = \frac{-a_2^2 b_1^2 c_1^2 c_2^2}{M_1^3 M_2^3 M_3} \left[ a_3^2 \left( c_2^2 M_1 \sin 2\alpha_3 + (b_1^2 + c_1^2) M_2 \sin 2(\alpha_3 - \gamma_2) \right) - ((b_1^2 + c_1^2) a_2^2 + b_1^2 c_2^2) M_3 \sin 2\gamma_2 \right]. \quad (32)$$

It follows that the leptogenesis phase is related to the low energy Dirac phase when the conditions

$$\left( (b_1^2 + c_1^2) a_2^2 + b_1^2 c_2^2 \right) M_3 \gg a_3^2 \left| c_2^2 M_1 \sin 2\alpha_3 \right|, \quad a_3^2 \left| (b_1^2 + c_1^2) M_2 \sin 2(\alpha_3 - \gamma_2) \right| \quad (33)$$

are fulfilled. Similar considerations can be made for all other textures in category (i). Note that in the basis that we are working, the Dirac mass matrix from the example in Eq. (27) contains only two physical phases, which is one less than the number of low energy phases in  $m_\nu$ . This facilitates the connection of low and high energy CP violation. We stress here that *all* four zero textures contain two physical phases. For this reason all 72 candidates have – in analogy to the conditions in Eq. (33) – the possibility [6] that the low energy leptonic CP violating phases are the ones responsible for leptogenesis.

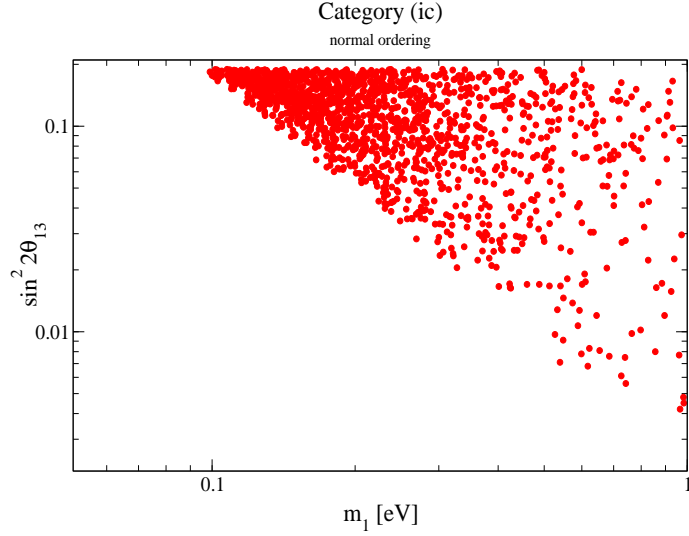


Figure 2: Category (ic) or  $(m_\nu)_{23} = 0$ : scatter plot of  $\sin^2 \theta_{13}$  versus the smallest mass in case of a normal mass ordering.

Let us next discuss the neutrino mixing properties of category (i), in which case the low energy neutrino mass matrix contains a vanishing off-diagonal entry. The phenomenology of mass matrices  $m_\nu$  having one single texture zero was analyzed in Ref. [28]. Consider first the case of  $(m_\nu)_{12} = 0$ , i.e., category (ia). The first thing to note is that zero  $U_{e3}$  is incompatible with the condition of vanishing  $(m_\nu)_{12}$  [28]. To elaborate, expanding in terms of  $|U_{e3}|$  one finds

$$(m_\nu)_{12} = (m_2 e^{2i\alpha} - m_1) \cos \theta_{12} \sin \theta_{12} \cos \theta_{23} + e^{i\delta} \sin \theta_{23} (e^{2i\beta} m_3 - \sin^2 \theta_{12} m_2 e^{2i\alpha} - \cos^2 \theta_{12} m_1) |U_{e3}|, \quad (34)$$

plus higher order terms of  $|U_{e3}|$ . The magnitude of the bracketed part of the zeroth order term is bounded from below roughly by  $\sqrt{\Delta m_\odot^2}$  for a normal hierarchy, by  $\frac{1}{2} \Delta m_\odot^2 / \sqrt{\Delta m_A^2}$  for an inverted hierarchy and by  $\frac{1}{2} \Delta m_\odot^2 / m_0$  for quasi-degenerate neutrinos with an average mass  $m_0$ . The 12-element therefore cannot vanish for  $U_{e3} = 0$ , but can vanish if  $U_{e3}$  departs from zero. It is clear from the above expression that in case of an inverted hierarchy and for quasi-degenerate neutrinos the bracketed part of the zeroth order term in Eq. (34) has to be small in order to allow the term of order  $\theta_{13}$  to cancel it. This in turn means that  $\sin \alpha$  has to be close to zero. In this case there are almost no cancellations in the effective mass  $\langle m \rangle = |(m_\nu)_{11}|$  governing neutrinoless double beta decay and we have

$$\langle m \rangle \simeq \sqrt{\Delta m_A^2} \cos^2 \theta_{13} \quad \text{inverted hierarchy,} \\ m_0 \cos^2 \theta_{13} \leq \langle m \rangle \leq m_0 \quad \text{quasi-degeneracy.} \quad (35)$$

The above value and range have to be compared with the lower limits, arising from maximal effects of Majorana phases, i.e.,  $\langle m \rangle_{\min} \simeq \cos^2 \theta_{13} \cos 2\theta_{12} \sqrt{\Delta m_A^2}$  and  $\langle m \rangle_{\min} \simeq$

$\cos^2 \theta_{13} \cos 2\theta_{12} m_0$ , respectively. The left panel of Fig. 1 shows for category (ia) a scatter plot of the effective mass versus the smallest mass in case of an inverted mass ordering. It is clearly seen that the largest possible values of  $\langle m \rangle$  are mostly populated. We also show in the right panel a scatter plot of  $\sin^2 2\theta_{13}$  versus the smallest mass for a normal mass ordering. In order to generate this and other plots to be presented later, we have varied all neutrino parameters within their allowed  $3\sigma$ -ranges quoted in Eq. (4). The results for category (ib), i.e.,  $(m_\nu)_{13} = 0$ , are basically identical to the ones for category (ia) [28]. Formally one can obtain the 13-entry of  $m_\nu$  from the 12-entry by replacing in the latter  $\sin \theta_{23}$  with  $\cos \theta_{23}$  and  $\cos \theta_{23}$  with  $-\sin \theta_{23}$ .

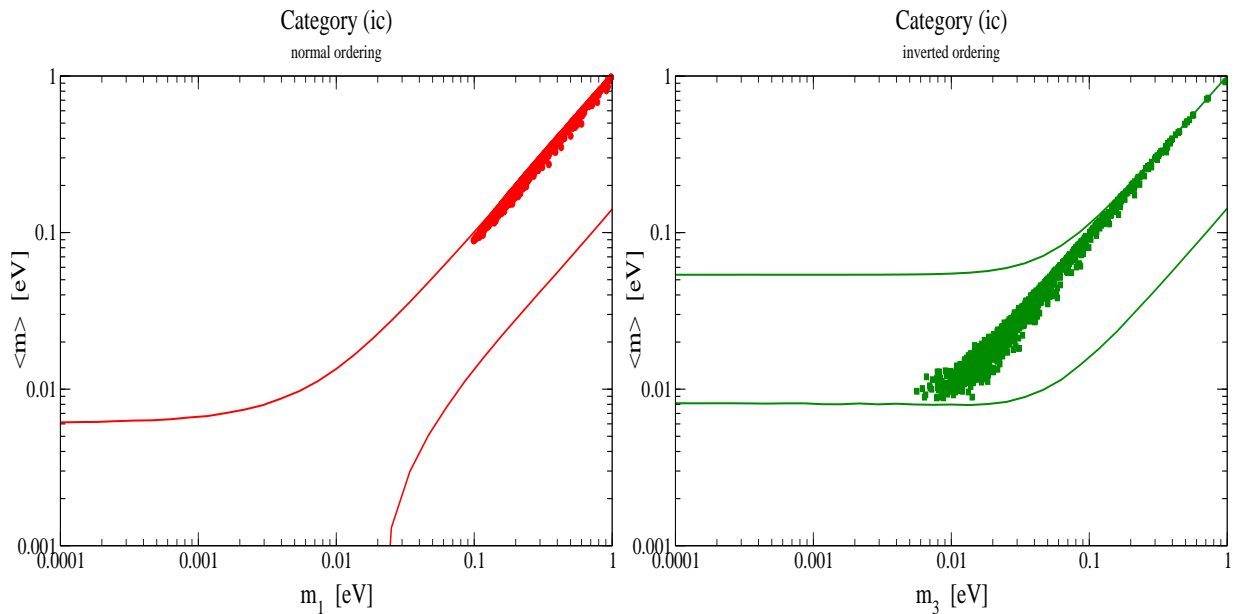


Figure 3: Category (ic) or  $(m_\nu)_{23} = 0$ : scatter plots of the effective mass versus the smallest in case of a normal mass ordering (left) and an inverted ordering (right). We have also given the general upper and lower limits of the effective mass when the currently allowed  $3\sigma$  values of the oscillation parameters are used.

Turning to category (ic), it can be shown that, for  $\theta_{13} = 0$  and a normal mass ordering, the 23-element of  $m_\nu$  cannot vanish unless neutrino masses are above several eV [28]. Fig. 2 illustrates this by showing the distribution of the smallest mass against  $\sin^2 2\theta_{13}$  in case of a normal mass ordering. For quasi-degenerate neutrinos, we can express the mass matrix element as

$$(m_\nu)_{23} \simeq -m_0 \cos \theta_{23} \sin \theta_{23} \left( (e^{2i\alpha} \cos^2 \theta_{12} + \sin^2 \theta_{12}) - e^{2i(\beta+\delta)} \right),$$

where for simplicity we have also set  $\theta_{13}$  to zero. It is clear that, in order to make  $(m_\nu)_{23}$  vanish, the expression in the brackets should be very small, or that the relations  $\sin \alpha \simeq \sin(\beta + \delta) \simeq 0$  should hold. This leads again to little cancellation in the effective

mass, as is obvious from Fig. 3.

We close this Section by commenting on the possibility that more than one entry of the low energy mass matrix vanishes. In this respect it is known that, in the mass diagonal charged lepton basis, two is the maximum number of vanishing elements allowed in the neutrino mass matrix [29]. We refer to Ref. [29] for details on the phenomenology of these cases. It is sufficient to note here that seven of those cases exist, namely the simultaneous vanishing of the 11- and 12-, the 11- and 13-, the 12- and 22-, the 13- and 22-, the 13- and 33-, the 12- and 33-, and finally the 22- and 33-entries. In category (ia), in which  $(m_\nu)_{12} = 0$ , there is the possibility that in addition  $(m_\nu)_{11}$ ,  $(m_\nu)_{22}$  or  $(m_\nu)_{33}$  can be zero. This in turn means that the branching ratios of the decays  $\tau \rightarrow e\gamma$  and  $\tau \rightarrow \mu\gamma$ , which depend on  $|(m_\nu)_{13}|^2$  and  $|(m_\nu)_{23}|^2$ , respectively, are guaranteed to be non-zero. The same is true for category (ib), in which case  $(m_\nu)_{13} = 0$ , and for which again only  $(m_\nu)_{11}$ ,  $(m_\nu)_{22}$  or  $(m_\nu)_{33}$  can be zero.  $\text{BR}(\mu \rightarrow e\gamma)$  and  $\text{BR}(\tau \rightarrow \mu\gamma)$  then are non-zero because there are proportional to the non-zero  $|(m_\nu)_{12}|^2$  and  $|(m_\nu)_{23}|^2$ , respectively. In case of category (ic), or  $(m_\nu)_{23} = 0$ , it turns out that no other mass matrix element can vanish, and therefore  $\text{BR}(\mu \rightarrow e\gamma)$  and  $\text{BR}(\tau \rightarrow e\gamma)$  are necessarily non-zero.

### 3.2 Category (ii)

Now, let us similarly consider the subclass of category (ii) in which columns  $l$  and  $k$  ( $\neq l$ ) are orthogonal, element by element. For this subclass of four zero textures, the relation

$$(m_D^\dagger m_D)_{lk} = 0 \quad (36)$$

applies. This means that the terms  $\mathcal{I}_{lk}^\alpha$  and  $\varepsilon_l$  vanish in the respective flavored and unflavored heavy neutrino decay asymmetries, cf. Eqs. (9) and (12).

It will be illuminating to explicitly see the different seesaw induced physical effects that appear in a given subclass of textures. Table 1 has been made for this purpose by considering category (iia). The leftmost column contains the Dirac mass matrices for particular textures of this category after one phase per row has been rotated away. This is followed in subsequent columns by expressions for only those heavy neutrino decay asymmetries which are nonzero and contribute accordingly to leptogenesis as well as their corresponding wash-out factors. For simplicity, we work as before under the assumption that  $M_1 \ll M_{2,3}$  so that one needs to consider only the decay of  $N_1$ , i.e.,  $i$  is always 1. However, this is an inessential assumption. Our tables can easily be generalized to the cases with  $j \neq i$ . Interestingly, we find again that the  $\mathcal{J}_1^\alpha$  are all zero. The entries in the last column of Table 1 are expressions describing the invariant  $J_{\text{CP}}$  relevant to CP violation that can be observed in neutrino oscillations. The latter is always the sum of three terms and we have chosen not to list common proportionality factors. Again, in analogy to the discussion in the previous Subsection, a comparison of the entries in the leptogenesis and the  $J_{\text{CP}}$  columns is instructive. It shows how there could be a one-to-one correspondence between the leptogenesis phase and the low energy Dirac phase  $\delta$ . For instance, consider the first row in

Table 1, for which only  $\varepsilon_1^\tau$  contributes to leptogenesis, and for which the CP phase denoted by  $\gamma_1$  is crucial. The same phase can control low energy (Dirac) CP violation provided the condition

$$b_2^2 M_1 M_3 \gg |c_1^2 M_2 M_3 \sin 2\beta_2|, |(a_3^2 + b_3^2 + c_3^2) M_1 M_2 \sin 2(\beta_2 - \gamma_1)| \quad (37)$$

is fulfilled. In the last two rows of Table 1 there are two nonzero decay asymmetries, which lead to more possibilities. In this respect, one may note that hierarchical heavy neutrinos lead to a suppression of  $\mathcal{I}_{13}^\alpha$  with respect to  $\mathcal{I}_{12}^\alpha$  by a factor  $M_2/M_3$ . Tables 2 and 3 show the leptogenesis related phenomenology of categories (iib) and (iic), respectively. The matrices can be obtained from the ones of category (iia) by interchanging the first with the second (first with the third) row.

Even though none of the branching ratios is guaranteed to vanish in this class of textures, there exists an interesting feature. For all 18 matrices in category (ii) the following relation applies for  $i \neq j$ :

$$|(m_D L m_D^\dagger)_{ij}| \propto |(m_\nu)_{ij}|, \quad (38)$$

i.e., the branching ratios for the decays  $\ell_i \rightarrow \ell_j \gamma$  are proportional to the square of the modulus of the  $ij$  element of the low energy mass matrix. This is similar to the situation in category (i). The crucial difference is however that in category (ii) the ratios of branching ratios are related to ratios of neutrino mass matrix elements without any ambiguity coming from the unknown values of the heavy Majorana neutrino masses. Consider again the example from the first row of Table 1. The low energy Majorana mass matrix is given as

$$m_\nu = - \begin{pmatrix} \frac{a_3^2}{M_3} & \frac{a_3 b_3}{M_3} & \frac{a_3 c_3}{M_3} \\ \cdot & \frac{b_2^2 e^{2i\beta_2}}{M_2} + \frac{b_3^2}{M_3} & \frac{b_3 c_3}{M_3} \\ \cdot & \cdot & \frac{c_1^2 e^{2i\gamma_1}}{M_1} + \frac{c_3^2}{M_3} \end{pmatrix}. \quad (39)$$

The relevant expressions for LFV are found to be

$$|(m_D L m_D^\dagger)_{12}|^2 = a_3^2 b_3^2 L_3^2, \quad |(m_D L m_D^\dagger)_{13}|^2 = a_3^2 c_3^2 L_3^2 \quad \text{and} \quad |(m_D L m_D^\dagger)_{23}|^2 = b_3^2 c_3^2 L_3^2.$$

Therefore, the ratios of branching ratios are unambiguously given by the ratios of the corresponding mass matrix elements. This ‘‘minimal lepton flavor violation’’ scenario in principle allows one to predict the rates from measurable low energy mass matrix elements. Indeed, from Eq. (7), we see that the following relations now hold in category (iia):

$$\frac{\text{BR}(\tau \rightarrow e\gamma)}{\text{BR}(\tau \rightarrow \mu\gamma)} \simeq \left| \frac{(m_\nu)_{13}}{(m_\nu)_{23}} \right|^2, \quad (40)$$

$$\frac{\text{BR}(\mu \rightarrow e\gamma)}{\text{BR}(\tau \rightarrow e\gamma)} \simeq \frac{1}{\text{BR}(\tau \rightarrow e\nu\bar{\nu})} \left| \frac{(m_\nu)_{12}}{(m_\nu)_{13}} \right|^2.$$

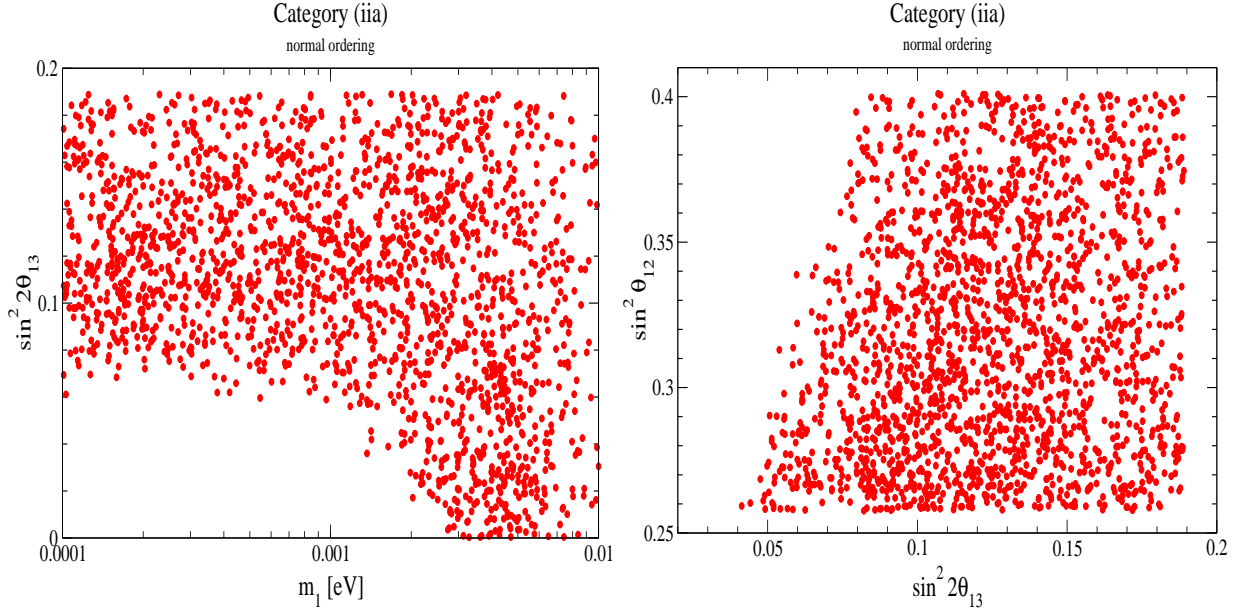


Figure 4: Category (iia): scatter plots of  $\sin^2 2\theta_{13}$  versus the smallest mass  $m_1$  and of  $\sin^2 2\theta_{12}$  versus  $\sin^2 \theta_{13}$  (for  $m_1 = 0.001$  eV) in case of a normal mass ordering and when the conditions  $|(m_\nu)_{11} (m_\nu)_{23}| = |(m_\nu)_{12} (m_\nu)_{13}|$  and  $\text{Im}\{(m_\nu)_{11} (m_\nu)_{23} (m_\nu)_{12}^* (m_\nu)_{13}^*\} = 0$  are fulfilled.

Eq. (40) is valid for all textures of category (ii).

The three sub-categories in category (ii) have in addition correlations between the low energy mass matrix elements, given in Eqs. (20, 21, 22), which lead to

$$\frac{\text{BR}(\tau \rightarrow e\gamma)}{\text{BR}(\tau \rightarrow \mu\gamma)} \simeq \left| \frac{(m_\nu)_{13}}{(m_\nu)_{23}} \right|^2 = \begin{cases} \left| \frac{(m_\nu)_{11}}{(m_\nu)_{12}} \right|^2 & \text{category (iia)}, \\ \left| \frac{(m_\nu)_{12}}{(m_\nu)_{22}} \right|^2 & \text{category (iib)}, \\ \left| \frac{(m_\nu)_{12} (m_\nu)_{33}}{(m_\nu)_{23}^2} \right|^2 & \text{category (iic)} \end{cases} \quad (41)$$

and

$$\frac{\text{BR}(\mu \rightarrow e\gamma)}{\text{BR}(\tau \rightarrow e\gamma)} \text{BR}(\tau \rightarrow e\nu\bar{\nu}) \simeq \left| \frac{(m_\nu)_{12}}{(m_\nu)_{13}} \right|^2 = \begin{cases} \left| \frac{(m_\nu)_{11} (m_\nu)_{23}}{(m_\nu)_{13}^2} \right|^2 & \text{category (iia)}, \\ \left| \frac{(m_\nu)_{22}}{(m_\nu)_{23}} \right|^2 & \text{category (iib)}, \\ \left| \frac{(m_\nu)_{23}}{(m_\nu)_{33}} \right|^2 & \text{category (iic)}. \end{cases} \quad (42)$$

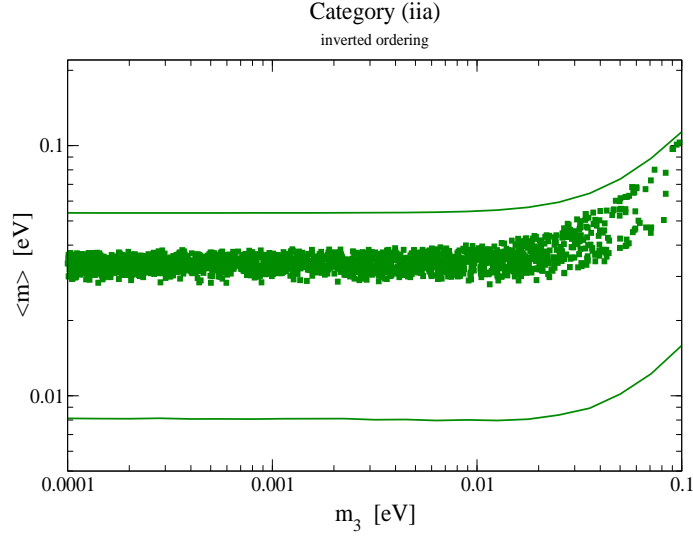


Figure 5: Category (iia): scatter plot of the effective mass  $\langle m \rangle$  versus the smallest mass  $m_3$  in case of an inverted mass ordering and when the conditions  $|(m_\nu)_{11} (m_\nu)_{23}| = |(m_\nu)_{12} (m_\nu)_{13}|$  and  $\text{Im}\{(m_\nu)_{11} (m_\nu)_{23} (m_\nu)_{12}^* (m_\nu)_{13}^*\} = 0$  are fulfilled. The solid (green) lines correspond to the upper and lower limit of the effective mass when the currently allowed  $3\sigma$  ranges of the oscillation parameters are used.

Because the neutrino mass matrix obeys  $\mu$ - $\tau$  (or 2-3) symmetry to a good approximation,  $|(m_\nu)_{12}/(m_\nu)_{13}|^2$  is typically 1. Therefore,  $\text{BR}(\tau \rightarrow e\gamma) \simeq 0.178 \text{BR}(\mu \rightarrow e\gamma)$ . With the current upper limit of  $1.2 \times 10^{-11}$  on  $\text{BR}(\mu \rightarrow e\gamma)$ , and an expected improvement of at most two orders of magnitude on the limit of  $\text{BR}(\tau \rightarrow e\gamma) \leq 1.1 \times 10^{-7}$ , it follows that in this scenario  $\tau \rightarrow e\gamma$  will probably not be observed in a foreseeable future. Since it turns out that  $\text{BR}(\tau \rightarrow \mu\gamma) \sim \text{BR}(\tau \rightarrow e\gamma)$ , the same is true for the decay  $\tau \rightarrow \mu\gamma$ . To discuss further the phenomenology of category (iia), we show in Fig. 4 scatter plots for a normal mass ordering in case the correlation (20) holds. Obtaining analytical correlations for this example is very complicated. If we set  $m_1 = \theta_{13} = 0$  and  $\theta_{23} = \pi/4$ , then Eq. (20) leads to  $\frac{1}{2} \sqrt{\Delta m_A^2 / \Delta m_\odot^2} = \cos^2 \theta_{12} \cos 2(\alpha - \beta - \delta) < 1$ , which is incompatible with the available data. This implies the presence of a lower limit on  $\sin^2 2\theta_{13}$ , which indeed turns out to be roughly 0.04 (0.06) for  $m_1 = 0.001$  (0) eV. This lower limit vanishes when the neutrino mass increases, which can clearly be seen in Fig. 4.

With regard to an inverted mass hierarchy, we find no correlation for the neutrino oscillation parameters. Instead, the effective mass  $\langle m \rangle = |(m_\nu)_{11}|$  governing neutrinoless double beta decay is constrained by the correlation in Eq. (20). Note that in the definition of the correlation for category (iia) the effective mass  $((m_\nu)_{11})$  appears explicitly. The influence on  $\langle m \rangle$  can be estimated by considering the equality  $|(m_\nu)_{11} (m_\nu)_{23}|^2 = |(m_\nu)_{21} (m_\nu)_{13}|^2$  in an approximate manner. Neglecting  $m_3$ , setting  $m_2 \simeq m_1 \simeq \sqrt{\Delta m_A^2}$ , and inserting

$\sin^2 \theta_{23} = \frac{1}{2}$ , we obtain from it the condition

$$\frac{(\Delta m_A^2)^2}{4} (1 - 2 \sin^2 2\theta_{12} \sin^2 \alpha) + \mathcal{O}(|U_{e3}|^2) \stackrel{!}{=} 0.$$

Hence,  $\sin^2 \alpha \simeq 1/(8 \sin^2 \theta_{12} \cos^2 \theta_{12})$  (which is equal to  $\frac{9}{16}$  if  $\sin^2 \theta_{12} = \frac{1}{3}$ ) and inserting this in the effective mass leads to

$$\langle m \rangle \simeq \frac{\cos^2 \theta_{13}}{\sqrt{2}} \sqrt{\Delta m_A^2}. \quad (43)$$

This has to be compared with the general lower and upper limits on  $\langle m \rangle$ , which are  $\cos 2\theta_{12} \cos^2 \theta_{13} \sqrt{\Delta m_A^2}$  and  $\cos^2 \theta_{13} \sqrt{\Delta m_A^2}$ , respectively. Fig. 5 shows how the effective mass as a function of the smallest mass  $m_3$  has considerably less spread than without the correlation Eq. (20). For the other two conditions in Eqs. (21) and (22) we did not find any interesting correlations between the neutrino observables.

Turning to the ratios of branching ratios, Eqs. (41) and (42) are phenomenologically very interesting. In Fig. 6 we show as a function of  $\sin^2 \theta_{23}$ , the ratio of the branching ratios of  $\tau \rightarrow e\gamma$  and  $\tau \rightarrow \mu\gamma$  in the left panel and of  $\mu \rightarrow e\gamma$  and  $\tau \rightarrow e\gamma$  in the right panel. These numbers are equal to  $|(m_\nu)_{13}|^2/|(m_\nu)_{23}|^2$  and  $(|(m_\nu)_{12}|^2/|(m_\nu)_{13}|^2)/\text{BR}(\tau \rightarrow e\bar{\nu})$ , respectively. Note that, for normal ordering, the  $\mu$ - $\tau$  block of  $m_\nu$  is usually larger than the elements of the  $e$ -row, while for the inverted ordering case, all elements of  $m_\nu$  are of similar magnitude. This explains why in the left panel the predictions for the inverted ordering are higher compared to that for the normal ordering. In addition, since  $\text{BR}(\tau \rightarrow e\bar{\nu}) = 0.178$ , the ratios shown in the right panel are larger than those in the left panel. To be more specific, let us consider a simplified example. For inverted ordering, assuming  $\theta_{13} = m_3 = 0$ ,  $m_2 \simeq m_1$  and  $\sin^2 \theta_{12} = \frac{1}{3}$ , we obtain

$$\frac{|(m_\nu)_{13}|^2}{|(m_\nu)_{23}|^2} \simeq \frac{1}{\cos^2 \theta_{23}},$$

which explains the mild increase of this ratio as a function of  $\sin^2 \theta_{23}$  in the left panel of Fig. 6. On the other hand, the ratio  $\text{BR}(\mu \rightarrow e\gamma)/\text{BR}(\tau \rightarrow e\gamma)$  is seen to be proportional to  $\cot^2 \theta_{23}$  for the same set of assumptions. This therefore results in the decrease seen for inverted ordering in the right panel of Fig. 6. For normal ordering and with the same set of assumptions one can show that  $|(m_\nu)_{12}|^2/|(m_\nu)_{13}|^2 \propto \tan^2 \theta_{23}$ . This explains the increase of  $\text{BR}(\mu \rightarrow e\gamma)/\text{BR}(\tau \rightarrow e\gamma)$  with  $\sin^2 \theta_{23}$  in the right panel of Fig. 6. Note that, for the inverted mass ordering  $\text{BR}(\tau \rightarrow e\gamma) \sim \text{BR}(\tau \rightarrow \mu\gamma)$ , while  $\text{BR}(\mu \rightarrow e\gamma) \sim \text{BR}(\tau \rightarrow e\gamma)$  is true irrespective of the neutrino mass spectrum. Therefore, we do not expect  $\text{BR}(\tau \rightarrow e\gamma)$  to be observed in the forthcoming experiments [18]. Similarly for the inverted ordering, the predicted  $\text{BR}(\tau \rightarrow \mu\gamma)$  is not expected to be checked experimentally in the next generation experiments [18]. The scatter plots of  $\text{BR}(\mu \rightarrow e\gamma)/\text{BR}(\tau \rightarrow e\gamma)$  in all sub-categories of category (ii) look very similar and the other cases show no interesting correlations.

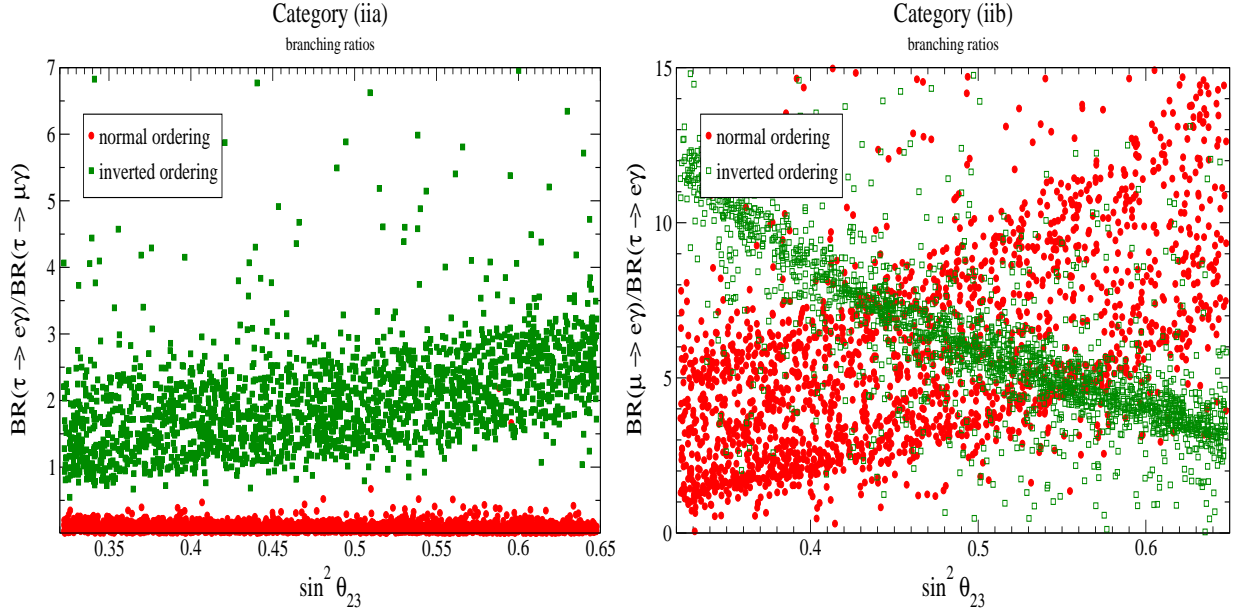


Figure 6: Category (iia): scatter plots of  $\text{BR}(\tau \rightarrow e\gamma)/\text{BR}(\tau \rightarrow \mu\gamma)$  (left) and  $\text{BR}(\mu \rightarrow e\gamma)/\text{BR}(\tau \rightarrow e\gamma)$  (right) against  $\sin^2 2\theta_{23}$  when the conditions  $|(m_\nu)_{11}(m_\nu)_{23}| = |(m_\nu)_{12}(m_\nu)_{13}|$  and  $\text{Im}\{(m_\nu)_{11}(m_\nu)_{23}(m_\nu)_{12}^*(m_\nu)_{13}^*\} = 0$  are fulfilled. The red circles are for the normal ordering, the green squares for the inverted one.

Finally, we discuss the possibility and implications of vanishing branching ratios, and hence the low energy mass matrix elements. Since the basic criteria for category (ii) comprise of zero sub-determinant conditions (cf. Eq. (20)-(22)), one can easily note that in this case, the vanishing of one element of  $m_\nu$  would necessitate the vanishing of another mass matrix element as well. Therefore, for category (ii) we cannot have just one zero  $m_\nu$  texture, and hence just one vanishing branching ratio. The allowed two zero textures of  $m_\nu$  have been extensively studied in the literature [29]. One can check that none of the phenomenologically viable two zero textures allow  $(m_\nu)_{23}$  to be zero. An immediate consequence of this is that for category (ii),  $\text{BR}(\tau \rightarrow \mu\gamma) \neq 0$ . Among the sub-categories, we note that for category (iia), if  $\text{BR}(\mu \rightarrow e\gamma) = 0$  (implying  $(m_\nu)_{12} = 0$ ), then  $(m_\nu)_{11} = 0$ . Therefore, for this case a vanishing  $\text{BR}(\mu \rightarrow e\gamma)$  predicts vanishing neutrinoless double beta decay – this in turn is possible only for normal mass ordering with  $m_1 \sim 0.005$  eV. For category (iib), the only allowed two zero texture is with  $(m_\nu)_{12} = 0$  and  $(m_\nu)_{22} = 0$ . For this category a vanishing  $(m_\nu)_{13}$  would make  $(m_\nu)_{12} = 0$  and this case is strongly disfavored by the data. Therefore,  $\text{BR}(\tau \rightarrow e\gamma) \neq 0$  for this case while  $\text{BR}(\mu \rightarrow e\gamma)$  could go to zero. On the other hand, for category (iic), the  $(m_\nu)_{12} \neq 0$  condition is imposed by the data, implying that  $\text{BR}(\mu \rightarrow e\gamma) \neq 0$ , while  $\text{BR}(\tau \rightarrow e\gamma)$  could go to zero if both  $(m_\nu)_{13} = 0$  and  $(m_\nu)_{22} = 0$  simultaneously.

## 4 Summary and Conclusions

We have looked at phenomenological constraints from the two maximally allowed categories of four zero textures in  $Y_\nu$  in the basis in which the mass matrices  $M_R$  and  $m_\ell$  are diagonal. Our framework is that of the supersymmetric type I seesaw and we have examined the consequences on seesaw parameters of the conditions imposed on elements of the neutrino Majorana mass matrix  $m_\nu$  by either category of textures. We have included the effective Majorana mass  $\langle m \rangle$ , appearing in neutrinoless nuclear double beta decay, in the list of seesaw parameters studied. Our use of those conditions is reliable in that the latter are radiatively stable, being invariant under RG running.

We have demonstrated via various scatter plots how restricted regions in the seesaw parameter space are selected by the said conditions. For the textures of each category, we have further derived a number of results on radiative LFV decays, several of them with observable consequences. For instance, any observation of the decay  $\ell_i \rightarrow \ell_j \gamma$  would rule out those category (i) textures which imply that  $(m_\nu)_{ij} = (m_\nu)_{ji}$  vanishes. In general, all 72 four zero textures predict that the branching ratios of  $\ell_i \rightarrow \ell_j \gamma$  are proportional to the absolute values squared of the mass matrix element  $(m_\nu)_{ij}$  times a function of heavy Majorana neutrino masses. For category (ii) this function is the same for all  $i, j$  and the ratios of branching ratios are directly given by ratios of low energy mass matrix elements. For category (ii), we have been able to generate sample scatter plots for ratios of branching ratios such as  $\text{BR}(\mu \rightarrow e\gamma)/\text{BR}(\tau \rightarrow e\gamma)$  and  $\text{BR}(\tau \rightarrow e\gamma)/\text{BR}(\tau \rightarrow \mu\gamma)$  against  $\sin^2\theta_{23}$ . We have also obtained results with physical consequences for leptogenesis from these textures. An example is that, for both categories (i) and (ii), we have derived conditions which fix the functional form of the leptogenesis phase purely in terms of the low energy Dirac phase without invoking any other phase from among the seesaw parameters. This is always possible for the four zero textures because their number of physical phases is two. We have also provided additional information by tabulating quantities relevant to lepton flavor asymmetries, wash-out factors and the Jarlskog invariant for each texture of category (ii).

In conclusion, we have highlighted the rich phenomenological structure of the allowed four zero textures in  $Y_\nu$  defined in the charged lepton and right-handed neutrino mass diagonal basis. The consequent conditions on  $m_\nu$  are radiatively stable. These have been shown to lead to significant reductions in the seesaw parameter space.

### Acknowledgments

We thank Michael Schmidt for helpful discussions. S.C. was supported by the XI Plan Neutrino Project at the Harish-Chandra Research Institute. W.R. was supported by the Deutsche Forschungsgemeinschaft in the Sonderforschungsbereich Transregio 27 “Neutrinos and beyond – Weakly interacting particles in Physics, Astrophysics and Cosmology” and

by the ERC under the Starting Grant MANITOP. P.R. was supported in part by the DAE BRNS of the Government of India and acknowledges the hospitality of the Harish-Chandra Research Institute. We also thank the organizers of WHEPP-X, where this work was initiated, for hospitality.

## References

- [1] S. Davidson and A. Ibarra, JHEP **0109**, 013 (2001) [arXiv:hep-ph/0104076]; J. R. Ellis, J. Hisano, S. Lola and M. Raidal, Nucl. Phys. B **621**, 208 (2002) [arXiv:hep-ph/0109125]; F. Deppisch, H. Päs, A. Redelbach, R. Rückl and Y. Shimizu, Eur. Phys. J. C **28**, 365 (2003) [arXiv:hep-ph/0206122]; J. R. Ellis and M. Raidal, Nucl. Phys. B **643**, 229 (2002) [arXiv:hep-ph/0206174]; S. Pascoli, S. T. Petcov and C. E. Yaguna, Phys. Lett. B **564**, 241 (2003) [arXiv:hep-ph/0301095]; S. Pascoli, S. T. Petcov and W. Rodejohann, Phys. Rev. D **68**, 093007 (2003) [arXiv:hep-ph/0302054]; W. Rodejohann, Eur. Phys. J. C **32**, 235 (2004) [arXiv:hep-ph/0311142]; S. T. Petcov, W. Rodejohann, T. Shindou and Y. Takanishi, Nucl. Phys. B **739**, 208 (2006) [arXiv:hep-ph/0510404]; F. Deppisch, H. Päs, A. Redelbach and R. Rückl, Phys. Rev. D **73**, 033004 (2006) [arXiv:hep-ph/0511062]; S. T. Petcov and T. Shindou, Phys. Rev. D **74**, 073006 (2006) [arXiv:hep-ph/0605151]; S. Antusch, E. Arganda, M. J. Herrero and A. M. Teixeira, JHEP **0611**, 090 (2006) [arXiv:hep-ph/0607263]; G. C. Branco, A. J. Buras, S. Jager, S. Uhlig and A. Weiler, JHEP **0709**, 004 (2007) [arXiv:hep-ph/0609067]; S. Antusch and A. M. Teixeira, JCAP **0702**, 024 (2007) [arXiv:hep-ph/0611232]; E. J. Chun, J. L. Evans, D. E. Morrissey and J. D. Wells, arXiv:0804.3050 [hep-ph]; M. Endo and T. Shindou, arXiv:0805.0996 [hep-ph]; S. Davidson, J. Garayoa, F. Palorini and N. Rius, arXiv:0806.2832 [hep-ph]; M. Hirsch, S. Kaneko and W. Porod, arXiv:0806.3361 [hep-ph].
- [2] P. Minkowski, Phys. Lett. B **67**, 421 (1977); M. Gell-Mann, P. Ramond, and R. Slansky, *Supergravity* (P. van Nieuwenhuizen et al. eds.), North Holland, Amsterdam, 1980, p. 315; T. Yanagida, in *Proceedings of the Workshop on the Unified Theory and the Baryon Number in the Universe* (O. Sawada and A. Sugamoto, eds.), KEK, Tsukuba, Japan, 1979, p. 95; S. L. Glashow, *The future of elementary particle physics*, in *Proceedings of the 1979 Cargèse Summer Institute on Quarks and Leptons* (M. Lévy et al. eds.), Plenum Press, New York, 1980, pp. 687; R. N. Mohapatra and G. Senjanović, Phys. Rev. Lett. **44**, 912 (1980).
- [3] P. H. Frampton, S. L. Glashow and D. Marfatia, Phys. Lett. B **536**, 79 (2002) [arXiv:hep-ph/0201008].
- [4] A. Ibarra and G. G. Ross, Phys. Lett. B **591**, 285 (2004) [arXiv:hep-ph/0312138].
- [5] S. Kaneko and M. Tanimoto, Phys. Lett. B **551**, 127 (2004) [arXiv:hep-ph/0210155].

- [6] G. C. Branco, R. Gonzalez Felipe, F. R. Joaquim, I. Masina, M. N. Rebelo and C. A. Savoy, Phys. Rev. D **67**, 073025 (2005) [arXiv:hep-ph/0211001].
- [7] G. C. Branco, D. Emmanuel-Costa, M. N. Rebelo and P. Roy, Phys. Rev. D **77**, 053011 (2008) [arXiv:0712.0774 [hep-ph]].
- [8] M. C. Gonzalez-Garcia and M. Maltoni, Phys. Rept. **460**, 1 (2008) [arXiv:0704.1800 [hep-ph]].
- [9] G. L. Fogli *et al.*, arXiv:0805.2517 [hep-ph]; A. Bandyopadhyay, S. Choubey, S. Goswami, S. T. Petcov and D. P. Roy, arXiv:0804.4857 [hep-ph].
- [10] J. A. Casas and A. Ibarra, Nucl. Phys. B **618**, 171 (2001) [arXiv:hep-ph/0103065].
- [11] For a review on this framework and many references see W. Rodejohann, arXiv:0804.3925 [hep-ph].
- [12] F. Borzumati and A. Masiero, Phys. Rev. Lett. **57**, 961 (1986); J. Hisano, T. Moroi, K. Tobe and M. Yamaguchi, Phys. Rev. D **53**, 2442 (1996) [arXiv:hep-ph/9510309].
- [13] W. M. Yao *et al.* [Particle Data Group], J. Phys. G **33**, 1 (2006)
- [14] M. L. Brooks *et al.* [MEGA Collaboration], Phys. Rev. Lett. **83**, 1521 (1999) [arXiv:hep-ex/9905013].
- [15] B. Aubert *et al.* [BABAR Collaboration], Phys. Rev. Lett. **96**, 041801 (2006) [arXiv:hep-ex/0508012].
- [16] B. Aubert *et al.* [BABAR Collaboration], Phys. Rev. Lett. **95**, 041802 (2005) [arXiv:hep-ex/0502032].
- [17] See the homepage of the MEG experiment, <http://meg.web.psi.ch>.
- [18] A. G. Akeroyd *et al.*, arXiv:hep-ex/0406071.
- [19] J. Hisano, T. Moroi, K. Tobe and M. Yamaguchi, Phys. Rev. D **53**, 2442 (1996) [arXiv:hep-ph/9510309]; E. Arganda, M. J. Herrero and A. M. Teixeira, JHEP **0710**, 104 (2007) [arXiv:0707.2955 [hep-ph]]; S. Davidson, arXiv:0809.0263 [hep-ph].
- [20] M. Fukugita and T. Yanagida, Phys. Lett. B **174**, 45 (1986).
- [21] For a recent review, see S. Davidson, E. Nardi and Y. Nir, arXiv:0802.2962 [hep-ph].
- [22] L. Covi, E. Roulet and F. Vissani, Phys. Lett. B **384**, 169 (1996).
- [23] A. Abada *et al.*, JCAP **0604**, 004 (2006) [arXiv:hep-ph/0601083];
- [24] E. Nardi, Y. Nir, E. Roulet and J. Racker, JHEP **0601**, 164 (2006) [arXiv:hep-ph/0601084].

- [25] A. Abada, S. Davidson, A. Ibarra, F. X. Josse-Michaux, M. Losada and A. Riotto, JHEP **0609**, 010 (2006) [arXiv:hep-ph/0605281].
- [26] A. Ibarra and C. Simonetto, JHEP **0804**, 102 (2008) [arXiv:0802.3858 [hep-ph]].
- [27] See, e.g., S. Antusch, J. Kersten, M. Lindner and M. Ratz, Nucl. Phys. B **674**, 401 (2003) [arXiv:hep-ph/0305273]; S. Antusch, J. Kersten, M. Lindner, M. Ratz and M. A. Schmidt, JHEP **0503**, 024 (2005) [arXiv:hep-ph/0501272].
- [28] A. Merle and W. Rodejohann, Phys. Rev. D **73**, 073012 (2006) [arXiv:hep-ph/0603111].
- [29] P. H. Frampton, S. L. Glashow and D. Marfatia, Phys. Lett. B **536**, 79 (2002) [arXiv:hep-ph/0201008]; Z. Z. Xing, Phys. Lett. B **530**, 159 (2002) [arXiv:hep-ph/0201151]; B. R. Desai, D. P. Roy and A. R. Vaucher, Mod. Phys. Lett. A **18**, 1355 (2003) [arXiv:hep-ph/0209035].

$m_D =$	leptogenesis	wash-out	$J_{CP} \propto$
$\begin{pmatrix} 0 & 0 & a_3 \\ 0 & b_2 e^{i\beta_2} & b_3 \\ c_1 e^{i\gamma_1} & 0 & c_3 \end{pmatrix}$	$\mathcal{I}_{13}^\tau = -c_1^2 c_3^2 \sin 2\gamma_1$	$\tilde{m}_1^\tau = c_1^2/M_1$	$b_2^2 M_1 M_3 \sin 2\gamma_1 - c_1^2 M_2 M_3 \sin 2\beta_2$ $-(a_3^2 + b_3^2 + c_3^2) M_1 M_2 \sin 2(\beta_2 - \gamma_1)$
$\begin{pmatrix} 0 & 0 & a_3 \\ b_1 e^{i\beta_1} & 0 & b_3 \\ 0 & c_2 e^{i\gamma_2} & c_3 \end{pmatrix}$	$\mathcal{I}_{13}^\mu = -b_1^2 b_3^2 \sin 2\beta_1$	$\tilde{m}_1^\mu = b_1^2/M_1$	$b_1^2 M_2 M_3 \sin 2\gamma_2 - c_2^2 M_1 M_3 \sin 2\beta_1$ $-(a_3^2 + b_3^2 + c_3^2) M_1 M_2 \sin 2(\beta_1 - \gamma_2)$
$\begin{pmatrix} 0 & a_2 & 0 \\ 0 & b_2 e^{i\beta_2} & b_3 \\ c_1 e^{i\gamma_1} & c_2 & 0 \end{pmatrix}$	$\mathcal{I}_{12}^\tau = -c_1^2 c_2^2 \sin 2\gamma_1$	$\tilde{m}_1^\tau = c_1^2/M_1$	$c_1^2 M_2 M_3 \sin 2\beta_2 + b_3^2 M_1 M_2 \sin 2\gamma_1$ $+(a_2^2 + b_2^2 + c_2^2) M_1 M_3 \sin 2(\beta_2 + \gamma_1)$
$\begin{pmatrix} 0 & a_2 & 0 \\ b_1 & b_2 e^{i\beta_2} & 0 \\ 0 & c_2 & c_3 e^{i\gamma_3} \end{pmatrix}$	$\mathcal{I}_{12}^\mu = b_1^2 b_2^2 \sin 2\beta_2$	$\tilde{m}_1^\mu = b_1^2/M_1$	$b_1^2 M_2 M_3 \sin 2\gamma_3 + c_3^2 M_1 M_2 \sin 2\beta_2$ $+(a_2^2 + b_2^2 + c_2^2) M_1 M_3 \sin 2(\beta_2 + \gamma_3)$
$\begin{pmatrix} a_1 & 0 & 0 \\ b_1 & b_2 e^{i\beta_2} & 0 \\ c_1 & 0 & c_3 e^{i\gamma_3} \end{pmatrix}$	$\mathcal{I}_{12}^\mu = b_1^2 b_2^2 \sin 2\beta_2$ $\mathcal{I}_{13}^\tau = c_1^2 c_3^2 \sin 2\gamma_3$	$\tilde{m}_1^\mu = b_1^2/M_1$ $\tilde{m}_1^\tau = c_1^2/M_1$	$b_2^2 M_1 M_3 \sin 2\gamma_3 - c_3^2 M_1 M_2 \sin 2\beta_2$ $-(a_1^2 + b_1^2 + c_1^2) M_2 M_3 \sin 2(\beta_2 - \gamma_3)$
$\begin{pmatrix} a_1 & 0 & 0 \\ b_1 e^{i\beta_1} & 0 & b_3 \\ c_1 & c_2 e^{i\gamma_2} & 0 \end{pmatrix}$	$\mathcal{I}_{13}^\mu = -b_1^2 b_3^2 \sin 2\beta_1$ $\mathcal{I}_{12}^\tau = c_1^2 c_2^2 \sin 2\gamma_2$	$\tilde{m}_1^\mu = b_1^2/M_1$ $\tilde{m}_1^\tau = c_1^2/M_1$	$b_3^2 M_1 M_2 \sin 2\gamma_2 + c_2^2 M_1 M_3 \sin 2\beta_1$ $+(a_1^2 + b_1^2 + c_1^2) M_2 M_3 \sin 2(\beta_1 + \gamma_2)$

Table 1: Category (iia): The Dirac mass matrix, the non-zero expressions relevant for leptogenesis and the corresponding wash-out factors, and the relevant part of the invariant for CP violation in neutrino oscillations. For this category at low energy the correlation  $|(m_\nu)_{11} (m_\nu)_{23}| - |(m_\nu)_{12} (m_\nu)_{13}| = \arg \{(m_\nu)_{11} (m_\nu)_{23} (m_\nu)_{12}^* (m_\nu)_{13}^*\} = 0$  applies.

$m_D =$	leptogenesis	wash-out	$J_{CP} \propto$
$\begin{pmatrix} 0 & a_2 e^{i\alpha_2} & a_3 \\ 0 & 0 & b_3 \\ c_1 e^{i\gamma_1} & 0 & c_3 \end{pmatrix}$	$\mathcal{I}_{13}^\tau = -c_1^2 c_3^2 \sin 2\gamma_1$	$\tilde{m}_1^\tau = c_1^2/M_1$	$a_2^2 M_1 M_3 \sin 2\gamma_1 - c_1^2 M_2 M_3 \sin 2\alpha_2$ $- (a_3^2 + b_3^2 + c_3^2) M_1 M_2 \sin 2(\alpha_2 - \gamma_1)$
$\begin{pmatrix} a_1 e^{i\alpha_1} & 0 & a_3 \\ 0 & 0 & b_3 \\ 0 & c_2 e^{i\gamma_2} & c_3 \end{pmatrix}$	$\mathcal{I}_{13}^e = -a_1^2 a_3^2 \sin 2\alpha_1$	$\tilde{m}_1^e = a_1^2/M_1$	$a_1^2 M_2 M_3 \sin 2\gamma_2 - c_2^2 M_1 M_3 \sin 2\alpha_1$ $- (a_3^2 + b_3^2 + c_3^2) M_1 M_2 \sin 2(\alpha_1 - \gamma_2)$
$\begin{pmatrix} 0 & a_2 e^{i\alpha_2} & a_3 \\ 0 & b_2 & 0 \\ c_1 e^{i\gamma_1} & c_2 & 0 \end{pmatrix}$	$\mathcal{I}_{12}^\tau = -c_1^2 c_2^2 \sin 2\gamma_1$	$\tilde{m}_1^\tau = c_1^2/M_1$	$a_3^2 M_1 M_2 \sin 2\gamma_1 + c_1^2 M_2 M_3 \sin 2\alpha_2$ $+ (a_2^2 + b_2^2 + c_2^2) M_1 M_3 \sin 2(\alpha_2 + \gamma_1)$
$\begin{pmatrix} a_1 & a_2 e^{i\alpha_2} & 0 \\ 0 & b_2 & 0 \\ 0 & c_2 & c_3 e^{i\gamma_3} \end{pmatrix}$	$\mathcal{I}_{12}^e = a_1^2 a_2^2 \sin 2\alpha_2$	$\tilde{m}_1^e = a_1^2/M_1$	$a_1^2 M_2 M_3 \sin 2\gamma_3 + c_3^2 M_1 M_2 \sin 2\alpha_2$ $+ (a_2^2 + b_2^2 + c_2^2) M_1 M_3 \sin 2(\alpha_2 + \gamma_3)$
$\begin{pmatrix} a_1 & a_2 e^{i\alpha_2} & 0 \\ b_1 & 0 & 0 \\ c_1 & 0 & c_3 e^{i\gamma_3} \end{pmatrix}$	$\mathcal{I}_{12}^e = a_1^2 a_2^2 \sin 2\alpha_2$ $\mathcal{I}_{13}^\tau = c_1^2 c_3^2 \sin 2\gamma_3$	$\tilde{m}_1^e = a_1^2/M_1$ $\tilde{m}_1^\tau = c_1^2/M_1$	$a_2^2 M_1 M_3 \sin 2\gamma_3 - c_3^2 M_1 M_2 \sin 2\alpha_2$ $- (a_1^2 + b_1^2 + c_1^2) M_2 M_3 \sin 2(\alpha_2 - \gamma_3)$
$\begin{pmatrix} a_1 e^{i\alpha_1} & 0 & a_3 \\ b_1 & 0 & 0 \\ c_1 & c_2 e^{i\gamma_2} & 0 \end{pmatrix}$	$\mathcal{I}_{13}^e = -a_1^2 a_3^2 \sin 2\alpha_1$ $\mathcal{I}_{12}^\tau = c_1^2 c_2^2 \sin 2\gamma_2$	$\tilde{m}_1^e = a_1^2/M_1$ $\tilde{m}_1^\tau = c_1^2/M_1$	$a_3^2 M_1 M_2 \sin 2\gamma_2 + c_2^2 M_1 M_3 \sin 2\alpha_1$ $+ (a_1^2 + b_1^2 + c_1^2) M_2 M_3 \sin 2(\alpha_1 + \gamma_2)$

Table 2: Category (iib): the Dirac mass matrix, the non-zero expressions relevant for leptogenesis and the corresponding wash-out factors, and the relevant part of the invariant for CP violation in neutrino oscillations. For this category at low energy the correlation  $|(m_\nu)_{22} (m_\nu)_{13}| - |(m_\nu)_{12} (m_\nu)_{23}| = \arg \{(m_\nu)_{22} (m_\nu)_{13} (m_\nu)_{12}^* (m_\nu)_{23}^*\} = 0$  applies.

$m_D =$	leptogenesis	wash-out	$J_{CP} \propto$
$\begin{pmatrix} a_1 e^{i\alpha_1} & 0 & a_3 \\ 0 & b_2 e^{i\beta_2} & b_3 \\ 0 & 0 & c_3 \end{pmatrix}$	$\mathcal{I}_{13}^e = -a_1^2 a_3^2 \sin 2\alpha_1$	$\tilde{m}_1^e = a_1^2/M_1$	$a_1^2 M_2 M_3 \sin 2\beta_2 - b_2^2 M_1 M_3 \sin 2\alpha_1$ $- (a_3^2 + b_3^2 + c_3^2) M_1 M_2 \sin 2(\alpha_1 - \beta_2)$
$\begin{pmatrix} 0 & a_2 e^{i\alpha_2} & a_3 \\ b_1 e^{i\beta_1} & 0 & b_3 \\ 0 & 0 & c_3 \end{pmatrix}$	$\mathcal{I}_{13}^\mu = -b_1^2 b_3^2 \sin 2\beta_1$	$\tilde{m}_1^\mu = b_1^2/M_1$	$a_2^2 M_1 M_3 \sin 2\beta_1 - b_1^2 M_2 M_3 \sin 2\alpha_2$ $- (a_3^2 + b_3^2 + c_3^2) M_1 M_2 \sin 2(\alpha_2 - \beta_1)$
$\begin{pmatrix} a_1 e^{i\alpha_1} & a_2 & 0 \\ 0 & b_2 e^{i\beta_2} & b_3 \\ 0 & c_2 & 0 \end{pmatrix}$	$\mathcal{I}_{12}^e = -a_1^2 a_2^2 \sin 2\alpha_1$	$\tilde{m}_1^e = a_1^2/M_1$	$a_1^2 M_2 M_3 \sin 2\beta_2 + b_3^2 M_1 M_2 \sin 2\alpha_1$ $+ (a_2^2 + b_2^2 + c_2^2) M_1 M_3 \sin 2(\alpha_1 + \beta_2)$
$\begin{pmatrix} 0 & a_2 & a_3 e^{i\alpha_3} \\ b_1 & b_2 e^{i\beta_2} & 0 \\ 0 & c_2 & 0 \end{pmatrix}$	$\mathcal{I}_{12}^\mu = b_1^2 b_2^2 \sin 2\beta_2$	$\tilde{m}_1^\mu = b_1^2/M_1$	$a_3^2 M_1 M_2 \sin 2\beta_2 + b_1^2 M_2 M_3 \sin 2\alpha_3$ $+ (a_2^2 + b_2^2 + c_2^2) M_1 M_3 \sin 2(\alpha_3 + \beta_2)$
$\begin{pmatrix} a_1 & 0 & a_3 e^{i\alpha_3} \\ b_1 & b_2 e^{i\beta_2} & 0 \\ c_1 & 0 & 0 \end{pmatrix}$	$\mathcal{I}_{13}^e = a_1^2 a_3^2 \sin 2\alpha_3$ $\mathcal{I}_{12}^\mu = b_1^2 b_2^2 \sin 2\beta_2$	$\tilde{m}_1^e = a_1^2/M_1$ $\tilde{m}_1^\mu = b_1^2/M_1$	$a_3^2 M_1 M_2 \sin 2\beta_2 - b_2^2 M_1 M_3 \sin 2\alpha_3$ $- (a_1^2 + b_1^2 + c_1^2) M_2 M_3 \sin 2(\alpha_3 - \beta_2)$
$\begin{pmatrix} a_1 & a_2 e^{i\alpha_2} & 0 \\ b_1 e^{i\beta_1} & 0 & b_3 \\ c_1 & 0 & 0 \end{pmatrix}$	$\mathcal{I}_{12}^e = a_1^2 a_2^2 \sin 2\alpha_2$ $\mathcal{I}_{13}^\mu = -b_1^2 b_3^2 \sin 2\beta_1$	$\tilde{m}_1^e = a_1^2/M_1$ $\tilde{m}_1^\mu = b_1^2/M_1$	$a_2^2 M_1 M_3 \sin 2\beta_1 + b_3^2 M_1 M_2 \sin 2\alpha_2$ $+ (a_1^2 + b_1^2 + c_1^2) M_2 M_3 \sin 2(\alpha_2 + \beta_1)$

Table 3: Category (iic): the Dirac mass matrix, the non-zero expressions relevant for leptogenesis and the corresponding wash-out factors, and the relevant part of the invariant for CP violation in neutrino oscillations. For this category at low energy the correlation  $|(m_\nu)_{33} (m_\nu)_{12}| - |(m_\nu)_{13} (m_\nu)_{32}| = \arg \{(m_\nu)_{33} (m_\nu)_{12} (m_\nu)_{13}^* (m_\nu)_{32}^*\} = 0$  applies.